JOURNAL OF AERONAUTICS AND SPACE TECHNOLOGIES
JULY 2016 VOLUME 9 NUMBER 2(35-45)

ATTITUDE GUIDANCE AND CONTROL, SIMULATION AND ANIMATION OF A LAND-SURVEY MINI-SATELLITE MOTION

Tatyana SOMOVA

Samara State Technical University
244 Molodogvardeyskaya Str. Samara 443100 Russia
te_somova@mail.ru

Received: *04th April 2016,* ***Accepted:*** *12th July 2016*

ABSTRACT
We present simple methods for attitude guidance and control of the land-survey mini-satellites, algorithms and software for simulation and animation of their spatial orbital motion.

Keywords*: remote sensing, mini-satellite, attitude guidance, control, simulation, animation*

MİNİ ARAZİ ÖLÇÜM UYDUSU YÖNELİMİNİN GÜDÜM VE KONTROLÜ, SİMÜLASYONU VE ANİMASYONU

ÖZ
Mini arazi ölçüm uydularının yöneliminin güdüm ve kontrolü için kolay yöntemler ile uzaysal yörünge hareketinin simülasyonu ve animasyonu için geliştirilen algoritmalar ve yazılımlar sunulmuştur.

Anahtar Kelimeler: *uzaktan algılama, mini-uydu, yönelim güdümü, kontrol, simülasyon, animasyon.*

1. INTRODUCTION

Problems of attitude guidance and control are actual for contemporary small information spacecraft (SC). The information mini-satellites today are applied for communication, geodesy, radio- and optoelectronic observation of the Earth at the orbit altitudes from 600 up to 1000 km, they have mass up to 500 kg and their structure contains the large-scale solar array panels (SAPs) for an energy supplying of the electro-mechanical drivers and magnetic torques. Studied the SC attitude control system (ACS) has the following standard executive equipment: electromechanical driver (ED) – cluster of four reaction wheels (RWs) by *General Electric* (*GE*) scheme with digital control and pulse-width controlled magnetic driver (MD) based on three current carrying coils whereby their magnetic torque vector interacts with geomagnetic field vector. The SC attitude determination system (ADS) is applied with the inertial measuring unit (IMU) corrected by the star tracker cluster (STC). In the paper we consider problems on the SC attitude guidance and digital control by the ED with its unloading by the MD and shortly present elaborated algorithms and software for simulation and animation of the land-survey mini-satellite motion, Fig. 1.

2. MODELS AND A PROBLEM STATEMENT

We consider a land-survey SC equipped with a telescope and matrices of optoelectronic converters (OECs) into its focal plane (FP). The matrices work in mode of the time delay and integration (TDI) during an optoelectronic observation of the Earth surface parts by a set of routes for their scanning. We have applied standard reference frames – inertial reference frame (IRF); Greenwich reference frame (GRF); geodesic horizon reference frame (HRF) with geodesic coordinates L, B and H; orbital reference frame (ORF) $Ox^{o}y^{o}z^{o}$ and SC body reference frame (BRF) $Oxyz$ with origin in its mass center O, Fig. 1. There are introduced the sensor reference frame (SRF), the image field reference fra-me (FRF) $O_i x^i y^i z^i$ with origin in center O_i of the FP and the visual (sight-

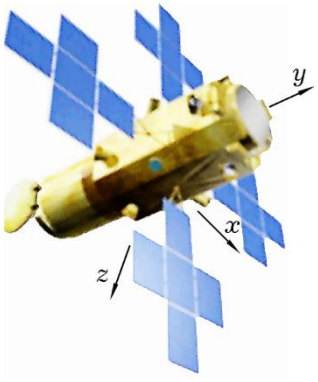

Figure 1. The *Sirius-1* SC

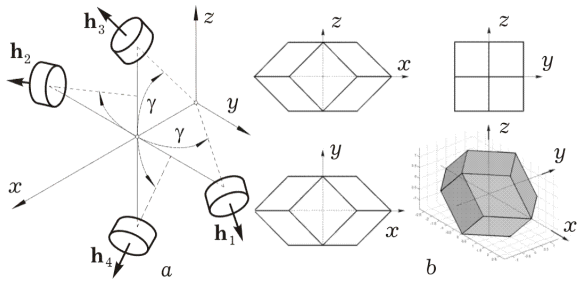

Figure 2. The *GE* scheme (*a*) and its AM envelope (*b*)

ing) reference frame (VRF) with origin in center O_v of main OEC linear array. A guidance law corresponds to a route observation when required motion of optical image is realized on surface of the OECs. In the BRF four RW rotation axes are arranged on the cone with angle γ, see Fig. 2. We use notations $\mathrm{col}(\cdot)=\{\cdot\}$, $\mathrm{line}(\cdot)=[\cdot]$, $(\cdot)^{\mathrm{t}}$, $[\mathbf{a}\times]$, $\mathrm{diag}\{\cdot\}=\lceil\cdot\rfloor$ and $\circ$, $\tilde{\circ}$ for vectors, matrices and quaternions. We introduce quaternion $\mathbf{\Lambda}^{\mathrm{o}}$ and angles by roll ϕ_1, yaw ϕ_2, pitch ϕ_3 of the BRF orientation with respect to the ORF. These angles are applied in sequence 312 for indexes $i=1,2,3\equiv 1\div 3\ \equiv x,y,z$. In the IRF the SC quaternion $\mathbf{\Lambda}=\mathbf{\Lambda}_{\mathrm{o}}\circ\mathbf{\Lambda}^{\mathrm{o}}$, where $\mathbf{\Lambda}_{\mathrm{o}}$ presents the ORF orientation in IRF. Quaternion $\mathbf{\Lambda}=(\lambda_0,\boldsymbol{\lambda})$, $\boldsymbol{\lambda}\equiv\{\lambda_i\}$ is one-one connected with vector $\boldsymbol{\sigma}=\{\sigma_i\}=\mathbf{e}\,\mathrm{tg}(\Phi/4)$ of Rodrigues modified parameters (RMP) by straight $\boldsymbol{\sigma}=\boldsymbol{\lambda}/(1+\lambda_0)$ and reverse $\lambda_0=(1-\sigma^2)/(1+\sigma^2)$; $\boldsymbol{\lambda}=2\boldsymbol{\sigma}/(1+\sigma^2)$ relations. Let us $\mathbf{\Lambda}^p(t)$ and $\boldsymbol{\omega}^p(t)$ present the SC attitude guidance law. Then quaternion $\mathbf{E}(t)\equiv(\mathrm{e}_0(t),\mathbf{e}(t))=\tilde{\mathbf{\Lambda}}^p(t)\circ\mathbf{\Lambda}(t)$, the attitude matrix $\mathbf{C}_{\mathrm{e}}=\mathbf{I}_3-2[\mathbf{e}\times]\mathbf{Q}_{\mathrm{e}}^{\mathrm{t}}$ with $\mathbf{Q}_{\mathrm{e}}\equiv\mathbf{I}_3\mathbf{e}_0+[\mathbf{e}\times]$ and column $\delta\boldsymbol{\phi}=\{\delta\phi_i\}=2\mathrm{e}_0\mathbf{e}$ present the attitude errors, and vector $\delta\boldsymbol{\omega}(t)=\{\delta\omega_i\}=\boldsymbol{\omega}(t)-\mathbf{C}_{\mathrm{e}}\boldsymbol{\omega}^p(t)$ is error on angular rate. The model of the SC motion is given as follows

$$\dot{\mathbf{\Lambda}}=\mathbf{\Lambda}\circ\boldsymbol{\omega}/2;\ \dot{\boldsymbol{\sigma}}=\tfrac{1}{4}(1-\sigma^2)\boldsymbol{\omega}+\tfrac{1}{2}\boldsymbol{\sigma}\times\boldsymbol{\omega}+\tfrac{1}{2}\boldsymbol{\sigma}<\boldsymbol{\sigma},\boldsymbol{\omega}>;$$

$$\begin{bmatrix}\mathbf{J}&\mathbf{D}_q&\mathbf{D}_r\\ \mathbf{D}_q^{\mathrm{t}}&\mathbf{A}^q&\mathbf{0}\\ \mathbf{D}_r^{\mathrm{t}}&\mathbf{0}&\mathbf{A}^r\end{bmatrix}\begin{bmatrix}\dot{\boldsymbol{\omega}}\\ \ddot{\mathbf{q}}\\ \dot{\boldsymbol{\Omega}}\end{bmatrix}=\begin{bmatrix}-[\boldsymbol{\omega}\times]\mathbf{G}+\mathbf{M}^{\mathrm{m}}+\mathbf{M}^{\mathrm{d}}\\ -\mathbf{A}^q(\mathbf{V}_q\dot{\mathbf{q}}+\mathbf{W}_q\mathbf{q})\\ \mathbf{m}-\mathbf{m}^{\mathrm{f}}\end{bmatrix};\quad(1)$$

$$\mathbf{A}_\gamma=\begin{bmatrix}C_\gamma&C_\gamma&C_\gamma&C_\gamma\\ S_\gamma&-S_\gamma&0&0\\ 0&0&S_\gamma&-S_\gamma\end{bmatrix};\ \begin{matrix}\mathbf{A}^r=J_r\mathbf{I}_4;\mathbf{D}_r=J_r\mathbf{A}_\gamma;\\ \mathbf{H}=\{\mathrm{H}_i\};\ \boldsymbol{\Omega}=\{\Omega_p\};\\ \mathbf{h}=\{\mathrm{h}_p\};\mathrm{h}_p=J_r\Omega_p;\end{matrix}$$

$\mathbf{G}=\mathbf{J}\boldsymbol{\omega}+\mathbf{H}+\mathbf{D}_q\dot{\mathbf{q}}$ is vector of the SC angular momentum (AM) in the BRF, columns $\mathbf{H}$ and $\mathbf{h}$ present the RW cluster and RW's AMs related as $\mathbf{H}=\mathbf{A}_\gamma\mathbf{h}$;

$C_\gamma=\cos\gamma,S_\gamma=\sin\gamma;\ \mathbf{m}=\{m_p\},\mathbf{m}^{\mathrm{f}}=\{m_p^{\mathrm{f}}\},p=1\div 4;$

$$\mathbf{A}^q=\lceil\mu_j\rfloor;\quad\mathbf{V}_q=\lceil\tfrac{\delta}{\pi}\omega_j^s\rfloor;\quad\mathbf{W}_q=\lceil(\omega_j^s)^2\rfloor;$$

vector of the MD torque $\mathbf{M}^{\mathrm{m}}=\{m_i^{\mathrm{m}}\}=-\mathbf{L}\times\mathbf{B}$, where the MD electromagnetic moment vector $\mathbf{L}=\{l_i\}$ has bounded components $|l_i|\le \mathrm{l}^{\mathrm{m}}$, and vector $\mathbf{B}=\mathrm{B}\mathbf{b}$ of the Earth magnetic induction with unit $\mathbf{b}$ are defined in the BRF; columns $\mathbf{m}$ and $\mathbf{m}^{\mathrm{f}}$ present the control and dry friction torques, and vector $\mathbf{M}^{\mathrm{d}}$ – disturbing torques. Each reaction wheel has limited resources on control torque and AM: $|m_p(t)|\le \mathrm{m}^{\mathrm{m}},|\mathrm{h}_p(t)|\le \mathrm{h}^{\mathrm{m}}$. The problems of the ADS signal processing are connected with integration of kinematic equations in using the information only on the quasi-coordinate increment vector obtained by IMU at availability of noises, calibration and alignment – identification and compensation of errors on a mutual angular position of the IMU and STC reference frames. Let the discrete measurements $\mathbf{\Lambda}_l=\mathbf{\Lambda}(t_l)$, $\boldsymbol{\omega}_l$ by ADS be fulfilled with period T_p, $l\in\mathrm{N}_0\equiv[0,1,2,..)$ and the RW rates $\Omega_{ps}=\Omega_p(t_s)$, $s\in\mathrm{N}_0$ be fulfilled with period T_q, forming of the RW digital control – with period $T_u\gg T_q$, and period of the MD pulse-width control is equal to $T_u^m\gg T_u$. First problem consists in synthesis of the SC attitude guidance laws and algorithms for discrete filtering, digital control of the RW cluster and also algorithms for the MD pulse-width control at unloading of the RW cluster, and second problem – in development of software for simulation and animation of a land-survey satellite spatial motion.

3. THE ATTITUDE GUIDANCE LAWS

Computing of quaternion $\mathbf{\Lambda}^p$, vectors of angular rate $\boldsymbol{\omega}^p$ and acceleration $\boldsymbol{\varepsilon}^p$ is carried out by a vector composition of all motions of the SRF in the GRF with careful taking into account both SC orbital and angular position, geodesic coordinates of observed terrestrial targets and lot of other factors. Les us $\boldsymbol{\omega}_{\mathrm{e}}^s$ and $\mathbf{v}_{\mathrm{e}}^s$ present vectors of angular rate and velocity of SC mass center in the SRF with respect to the GRF, matrix $\tilde{\mathbf{C}}=||\tilde{c}_{ij}||$ defines the SRF orientation respect to the HRF, function $D(t)$ presents an oblique range. For any point at the telescope FP longitudinal $\tilde{\tilde{y}}^i=\tilde{V}_y^i(\tilde{y}^i,\tilde{z}^i)$ and cross $\tilde{\tilde{z}}^i=\tilde{V}_z^i(\tilde{y}^i,\tilde{z}^i)$ components of normed image motion velocity (IMV) vector are calculated by relation

$$\begin{bmatrix}\tilde{\tilde{y}}^i\\ \tilde{\tilde{z}}^i\end{bmatrix}=\begin{bmatrix}\tilde{y}^i&1&0\\ \tilde{z}^i&0&1\end{bmatrix}\begin{bmatrix}q^i\tilde{\mathrm{v}}_{\mathrm{e}1}^s-\tilde{y}^i\omega_{\mathrm{e}3}^s+\tilde{z}^i\omega_{\mathrm{e}2}^s\\ q^i\tilde{\mathrm{v}}_{\mathrm{e}2}^s-\ \omega_{\mathrm{e}3}^s-\tilde{z}^i\omega_{\mathrm{e}1}^s\\ q^i\tilde{\mathrm{v}}_{\mathrm{e}3}^s+\ \omega_{\mathrm{e}2}^s+\tilde{y}^i\omega_{\mathrm{e}1}^s\end{bmatrix}.\quad(2)$$

Here $\tilde{y}^i = y^i / f_e$ and $\tilde{z}^i = z^i / f_e$ are normed focal coordinates of the point where f_e is the telescope focal distance, function $q^i = 1 - (\tilde{c}_{21}\tilde{y}^i + \tilde{c}_{31}\tilde{z}^i)/\tilde{c}_{11}$,

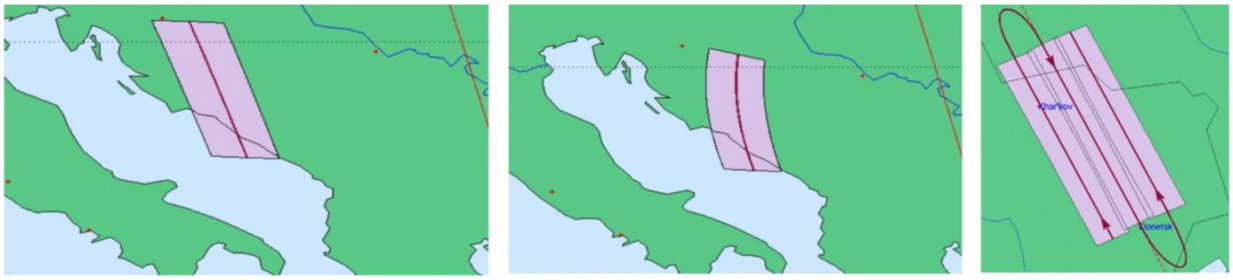

a *b* *c*

Figure 3. Examples of the scanning observation routes

and for SC mass center the vector of normed velocity has components $\tilde{v}^s_{ei} = v^s_{ei}(t)/D(t), i = 1 \div 3$. Relation (2) is applied for computing values of quaternion Λ^p_l and angular rate vector $\boldsymbol{\omega}^p_l$ in the time moments t_l for all types of scanning observation, moreover the optimal angular guidance laws are calculated by numerical integration of nonlinear kinematic equation for quaternion simultaneously with its strict concordance to an angular rate vector. We have concreted methods elaborated for trace routes, Fig. 3*a*; curved routes with equalization of the image longitudinal velocity (ILV), Fig. 3*b*; for an area land survey with sequence of orthodromic routes, Fig 3*c*, and also for obtaining stereo images of given terrestrial objects. Note that axis lines of orthodromic routes correspond to geodesic lines with given altitude over the Earth ellipsoid, i.e. here a scanning is fulfilled on an arch of "large geodesic circle" between the route points with given geodesic coordinates L, B, H. Let us consider a time interval $\mathrm{T} \equiv [0, T]$ of a scanning observation with following notations for its four points τ_p, $p = 1 \div 4$: $\tau_1 = 0$, $\tau_2 = T/3$, $\tau_3 = 2T/3$ and $\tau_4 = T$. For six values $\boldsymbol{\omega}_l = \boldsymbol{\omega}(t_l)$ near points $\tau_1 = 0, \tau_4 = T$ standard interpolation is carried out by the vector spline of five degree, that allows to calculate values $\boldsymbol{\varepsilon}_1 = \dot{\boldsymbol{\omega}}(\tau_1)$ and $\boldsymbol{\varepsilon}_4 = \dot{\boldsymbol{\omega}}(\tau_4)$ of angular acceleration vector. For four points $\tau_p \in \mathrm{T}$ values $\boldsymbol{\sigma}_p$, $p = 1 \div 4$ are computing, and also values $\dot{\boldsymbol{\sigma}}_p$ and $\ddot{\boldsymbol{\sigma}}_p$, $p = 1,4$ for two boundary points. Interpolation of the RMP vector $\boldsymbol{\sigma}(t)$ $\forall t \in \mathrm{T}$ is carried out by the vector spline of 7 degree $\boldsymbol{\sigma}_a(t) = \Sigma_0^7 \mathbf{a}_s t^s$ with 8 column $\mathbf{a}_s \in \mathbf{R}^3$, $s = 0 \div 7$ of unknown coefficients, moreover

$$\dot{\boldsymbol{\sigma}}_a(t) = \Sigma_1^7 s\, \mathbf{a}_s t^{s-1}; \quad \ddot{\boldsymbol{\sigma}}_a(t) = \Sigma_2^7 s\,(s-1)\, \mathbf{a}_s t^{s-2}.$$

All columns $\mathbf{a}_s$ are defined by following relations:

(i) boundary conditions $\boldsymbol{\sigma}_a(0) = \boldsymbol{\sigma}_1$; $\dot{\boldsymbol{\sigma}}_a(0) = \dot{\boldsymbol{\sigma}}_1$; $\ddot{\boldsymbol{\sigma}}_a(0) = \ddot{\boldsymbol{\sigma}}_1$ result in $\mathbf{a}_0 = \boldsymbol{\sigma}_1$, $\mathbf{a}_1 = \dot{\boldsymbol{\sigma}}_1$ и $\mathbf{a}_2 = \ddot{\boldsymbol{\sigma}}_1 / 2$;

(ii) conditions $\boldsymbol{\sigma}_a(\tau_2) = \boldsymbol{\sigma}_2$; $\boldsymbol{\sigma}_a(\tau_3) = \boldsymbol{\sigma}_3$ result in $\mathbf{a}_3 + \mathbf{a}_4\tau_2 + \mathbf{a}_5\tau_2^2 + \mathbf{a}_6\tau_2^3 + \mathbf{a}_7\tau_2^4 = \mathbf{b}_3$, $\mathbf{a}_3 + \mathbf{a}_4\tau_3 + \mathbf{a}_5\tau_3^2 + \mathbf{a}_6\tau_3^3 + \mathbf{a}_7\tau_3^4 = \mathbf{b}_4$ at $\mathbf{b}_3 = \boldsymbol{\sigma}_2 - (\mathbf{a}_0 + \mathbf{a}_1\tau_2 + \mathbf{a}_2\tau_2^2)/\tau_2^3$ and $\mathbf{b}_4 = \boldsymbol{\sigma}_3 - (\mathbf{a}_0 + \mathbf{a}_1\tau_3 + \mathbf{a}_2\tau_3^2)/\tau_3^3$;

(iii) boundary conditions $\boldsymbol{\sigma}_a(T) = \boldsymbol{\sigma}_4$; $\dot{\boldsymbol{\sigma}}_a(T) = \dot{\boldsymbol{\sigma}}_4$; $\ddot{\boldsymbol{\sigma}}_a(T) = \ddot{\boldsymbol{\sigma}}_4$ result in the equations $\mathbf{a}_3 + \mathbf{a}_4\tau_4 + \mathbf{a}_5\tau_4^2 + \mathbf{a}_6\tau_4^3 + \mathbf{a}_7\tau_4^4 = \mathbf{b}_5$, $3\mathbf{a}_3 + 4\mathbf{a}_4\tau_4 + 5\mathbf{a}_5\tau_4^2 + 6\mathbf{a}_6\tau_4^3 + 7\mathbf{a}_7\tau_4^4 = \mathbf{b}_6$, $6\mathbf{a}_3 + 12\mathbf{a}_4\tau_4 + 20\mathbf{a}_5\tau_4^2 + 30\mathbf{a}_6\tau_4^3 + 42\mathbf{a}_7\tau_4^4 = \mathbf{b}_7$. where $\mathbf{b}_5 = \boldsymbol{\sigma}_4 - (\mathbf{a}_0 + \mathbf{a}_1\tau_4 + \mathbf{a}_2\tau_4^2)/\tau_4^3$, $\mathbf{b}_6 = \dot{\boldsymbol{\sigma}}_4 - (\mathbf{a}_1 + 2\mathbf{a}_2\tau_4)/\tau_4^2$ and $\mathbf{b}_7 = \ddot{\boldsymbol{\sigma}}_4 - 2\mathbf{a}_2/\tau_4$.

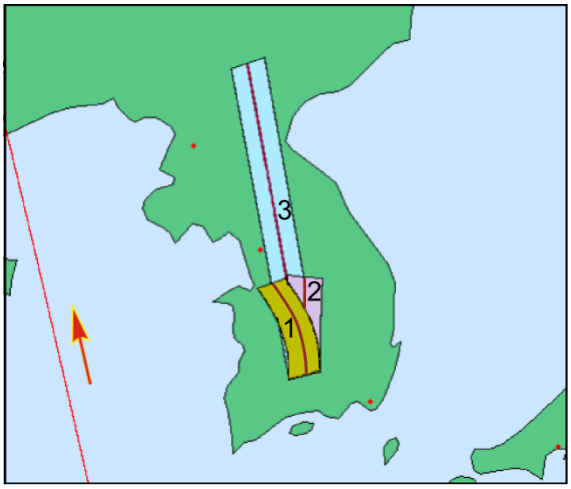

Figure 4. The observation routes on a map: 1 – with equalization of the ILV, 2 – orthodromic, 3 – trace.

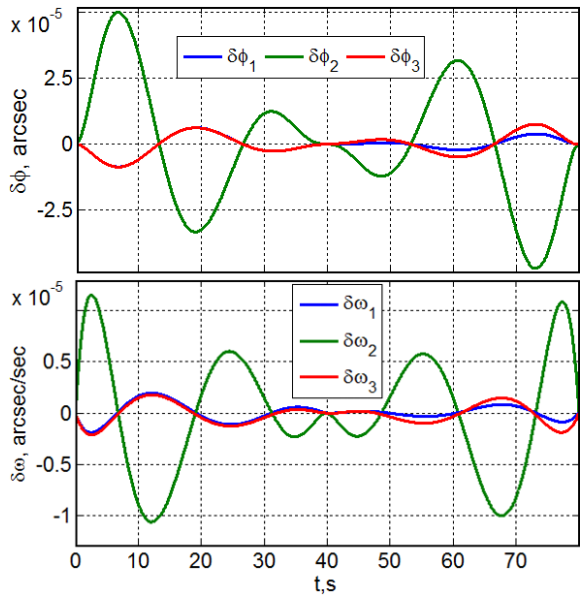

Figure 5. The interpolation errors at the trace route

For definition of 5 columns $\mathbf{a}_s$, $s=3\div7$ the matrix relation $\mathbf{AC}=\mathbf{B}$ is forming, where matrices $\mathbf{A}=[\mathbf{a}_3,\mathbf{a}_4,\mathbf{a}_5,\mathbf{a}_6,\mathbf{a}_7]$, $\mathbf{B}=[\mathbf{b}_3,\mathbf{b}_4,\mathbf{b}_5,\mathbf{b}_6,\mathbf{b}_7]$ and $\mathbf{C}=[\mathbf{c}_3,\mathbf{c}_4,\mathbf{c}_5,\mathbf{c}_6,\mathbf{c}_7]$ are composed from columns $\mathbf{a}_s$, $\mathbf{b}_s$, $\mathbf{c}_3=\mathbf{t}_2$, $\mathbf{c}_4=\mathbf{t}_3$, $\mathbf{c}_5=\mathbf{t}_4$, $\mathbf{c}_6=\mathbf{D}_6\mathbf{t}_4$, $\mathbf{c}_7=\mathbf{D}_7\mathbf{t}_4$ with columns $\mathbf{t}_p=\{1,\tau_p,\tau_p^2,\tau_p^3,\tau_p^4\}$, $p=2,3,4$ and matrices $\mathbf{D}_6=\lceil 3,4,5,6,7\rfloor$; $\mathbf{D}_7=\lceil 6,12,20,30,42\rfloor$. At last, all five columns $\mathbf{a}_s$, $s=3\div7$ are computing simultaneously by formula $[\mathbf{a}_3,\mathbf{a}_4,\mathbf{a}_5,\mathbf{a}_6,\mathbf{a}_7]=\mathbf{BC}^{-1}$. Verification of developed method was carried out, all indicated types of scanning observation were studied with respect to an interpolation accuracy for a land-survey SC on sun-synchronous orbit with altitude 600 km, Fig. 4. We obtained that maximum attitude errors are $\delta\phi^{\mathrm{m}}=\max|\delta\boldsymbol{\phi}|=0.03\,\mathrm{arc\ sec}$, $\delta\omega^{\mathrm{m}}=\max|\delta\boldsymbol{\omega}|=0.04$ arc sec/sec at a route duration $T\le 40$ sec. Developed method allows a smooth conjugation for adjacent parts of a guidance law on values of vectors $\boldsymbol{\sigma},\boldsymbol{\omega}$ and $\boldsymbol{\varepsilon}$ at scanning observation with arbitrary duration. Fig. 5 presents results on interpolation of the trace observation route with duration $T=80$ sec and smooth conjugation of two vector splines by 7 degree on the time intervals with duration $T=40$ s. The interpolation technology were presented in detail for a land-survey satellite attitude guidance at the scanning optoelectronic observations in paper [1].

At simplest modeling of the SC body with a telescope in the form of a free solid with an inertia tensor $\mathbf{J}$ the AM vector $\mathbf{G}^{\mathrm{o}}=\mathbf{J}\boldsymbol{\omega}+\mathbf{H}\equiv\mathbf{G}_0^{\mathrm{o}}$, where $\mathbf{G}_0^{\mathrm{o}}$ is a constant vector. Let us the SC ACS is balanced on the AM, e.g. $\mathbf{G}_0^{\mathrm{o}}\equiv\mathbf{0}$. Moreover model (1) of the SC dynamics is presented as $\dot{\boldsymbol{\omega}}=\boldsymbol{\varepsilon}$, where $\boldsymbol{\varepsilon}=\mathbf{J}^{-1}\mathbf{M}^{\mathrm{r}}$ is vector of angular acceleration, and model of the SC attitude motion has following kinematic representation

$$\dot{\boldsymbol{\Lambda}}(t)=\boldsymbol{\Lambda}(t)\circ\boldsymbol{\omega}(t)/2;\quad \dot{\boldsymbol{\omega}}(t)=\boldsymbol{\varepsilon}(t);\quad \boldsymbol{\varepsilon}^*(t)=\mathbf{v}. \quad (3)$$

In result analytical synthesis of the SC attitude guidance laws for two adjacent intervals of scanning observation the boundary conditions are known for rotational maneuver (RM) on quaternion $\boldsymbol{\Lambda}$, vectors $\boldsymbol{\omega}$, $\boldsymbol{\varepsilon}$ and also on vector $\boldsymbol{\varepsilon}^*$ at a time moment when second observation route is beginning. The spatial RMs are carried out for $t\in\mathrm{T_p}\equiv[t_0^p,t_{\mathrm{f}}^p]$, $t_{\mathrm{f}}^p\equiv t_0^p+T_p$ with general boundary conditions as follows

$$\begin{aligned}&\boldsymbol{\Lambda}(t_0^p)=\boldsymbol{\Lambda}_0;\ \boldsymbol{\omega}(t_0^p)=\boldsymbol{\omega};\ \boldsymbol{\varepsilon}(t_0^p)=\boldsymbol{\varepsilon}_0;\\ &\boldsymbol{\Lambda}(t_{\mathrm{f}}^p)=\boldsymbol{\Lambda}_{\mathrm{f}};\ \boldsymbol{\omega}(t_{\mathrm{f}}^p)=\boldsymbol{\omega}_{\mathrm{f}};\ \boldsymbol{\varepsilon}(t_{\mathrm{f}}^p)=\boldsymbol{\varepsilon}_{\mathrm{f}};\ \boldsymbol{\varepsilon}^*(t_{\mathrm{f}}^p)=\boldsymbol{\varepsilon}_{\mathrm{f}}^*.\end{aligned} \quad (4)$$

Modules of vectors $\boldsymbol{\omega}(t)$, $\boldsymbol{\varepsilon}(t)$, $\boldsymbol{\varepsilon}^*(t)$ are bounded, $|\boldsymbol{\omega}(t)|\le\overline{\omega}$, $|\boldsymbol{\varepsilon}(t)|\le\overline{\varepsilon}$ and $|\boldsymbol{\varepsilon}^*(t)|\le\overline{\varepsilon}^*$ because of limited envelopes of the RW cluster variation on the AM vector $\mathbf{H}$, the control torque vector $\mathbf{M}^{\mathrm{r}}=-\mathbf{H}^*$ and also permissible rate of its variation.

For integral energy criteria an approximate optimal spatial motion is based on necessary and sufficient condition for solvability of Darboux problem. Here solution is presented as result of composition by three simultaneously derived rotations of "embedded" bases $\mathbf{E}_k$ about units $\mathbf{e}_k$, $k=1,2,3$ of Euler axes, quaternion $\boldsymbol{\Lambda}$ is defined as $\boldsymbol{\Lambda}(t)=\boldsymbol{\Lambda}_0\circ\boldsymbol{\Lambda}_1(t)\circ\boldsymbol{\Lambda}_2(t)\circ\boldsymbol{\Lambda}_3(t)$ with $\boldsymbol{\Lambda}_k(t)=(\cos(\varphi_k(t)/2),\mathbf{e}_k\sin(\varphi_k(t)/2))$ and $\varphi_k(t)$ is angle of k's elementary rotation. Let us quaternion $\boldsymbol{\Lambda}^*\equiv(\lambda_0^*,\boldsymbol{\lambda}^*)=\widetilde{\boldsymbol{\Lambda}}_0\circ\boldsymbol{\Lambda}_{\mathrm{f}}$ has unit $\mathbf{e}_3=\boldsymbol{\lambda}^*/\sin(\varphi^*/2)$ of 3rd rotation where $\varphi^*=2\arccos(\lambda_0^*)$. For quaternions of 1st and 2nd rotations the boundary conditions $\boldsymbol{\Lambda}_1(t_{\mathrm{i}}^p)=\boldsymbol{\Lambda}_1(t_{\mathrm{f}}^p)=\boldsymbol{\Lambda}_2(t_{\mathrm{i}}^p)=\boldsymbol{\Lambda}_2(t_{\mathrm{f}}^p)=\mathbf{1}$ are applied, and for 3-rd rotation – conditions $\boldsymbol{\Lambda}_3(t_{\mathrm{i}}^p)=\mathbf{1}$, $\boldsymbol{\Lambda}_3(t_{\mathrm{f}}^p)=(\cos(\varphi_3^{\mathrm{f}}/2),\mathbf{e}_3\sin(\varphi_3^{\mathrm{f}}/2))$ where $\varphi_3^{\mathrm{f}}=\varphi^*$ and $\mathbf{1}$ – single quaternion. That corresponds to the angle values $\varphi_1^0=\varphi_1^{\mathrm{f}}=0$, $\varphi_2^0=\varphi_2^{\mathrm{f}}=0$ and $\varphi_3^9=0$. Units $\mathbf{e}_1$ and $\mathbf{e}_2$ of Euler axes by 1st and 2nd rotations, and also boundary conditions on angular rates $\dot{\varphi}_k^0,\dot{\varphi}_k^{\mathrm{f}}$ and angular accelerations $\ddot{\varphi}_k^0,\ddot{\varphi}_k^{\mathrm{f}}$, are defined from boundary conditions (4) for initial spatial problem (3) by explicit relations [2]. In result, approximate optimal solution of the problem is presented in explicit analytic form, where all angles of elementary rotations are splines by 5 degree of a time $t\in\mathrm{T_p}$.

Strict optimal spacecraft's RM for initial nonlinear problem (3) with boundary conditions (4) (without last condition) was numerically obtained by applying maximum principle and standard Newton iteration method. Moreover, analytical solution of the "start" problem (initial point) was applied in the form of approximate optimal motion. Iteration procedure uses the combine numerical integrations of direct and associat-

ed differential systems which are linearizated at neighbourhood of numerical solution on previous iteration. At such initial point the Newton's iteration process has a rapid convergence: usually there is needed only 2 – 3 iterations for obtaining a numerical solution with fine accuracy. Difference between approximate optimal and strict optimal control is very light – up to 5 % by functional for the SC practical rotational maneuvers with boundary conditions (4).

For smooth conjugation of the RM's right end with left border of a following route when scanning observation is fulfilled, applied analytic approximate optimization method allows availability of boundary condition $\boldsymbol{\varepsilon}^*(t_{\rm f}^p)=\boldsymbol{\varepsilon}_{\rm f}^*$ with given vector $\boldsymbol{\varepsilon}_{\rm f}^*$. Moreover all angles of elementary rotations are analytically carried out in the form of splines by six degree. Analytic procedure for calculation of approximate optimal motion is also elaborated at given restrictions $\overline{\omega}$, $\overline{\varepsilon}$ and $\boldsymbol{\varepsilon}^*(t)$ during the SC rotation maneuver. In this case the elementary rotation angles are obtained by carefully conjugation of splines with different degrees. Moreover difference between approximate optimal and strict optimal control is also light – up to 10 % on functional at practical width of a land-survey zone. On a map in Fig. 6 we present two routes and rotational maneuver between them for land-survey satellite on sun-synchronous orbit with altitude 600 km and longitude of ascending node $\Omega_{\rm o}=29.5$ deg. At a time reference from the moment of fly-over ascending node the synthesis was carried out of the attitude guidance laws for following data: (i) route 1 – trace scanning observation with duration $T^{(1)}=20$ sec beginning from the time moment $t_0^{(1)}=580$ sec at initial angles $\phi_1=-10$ deg and $\phi_3=0$ deg; (ii) rotational maneuver with duration $T_p=33$ sec beginning from the time moment $t_0^p=600$ sec for restrictions $\overline{\omega}=2$ deg/s, $\overline{\varepsilon}=1$ deg/s^2 and $\overline{\varepsilon}^*=1$ deg/s^3; (iii) route 2 – scanning observation with equalization of the ILV and duration $T^{(2)}=20$ sec beginning from the time moment $t_0^{(2)}=633$ sec and the observation point with longitude $L=18.11$ deg and latitude $B=39.68$ deg in the GRF at initial geodesic azimuth $A=+10$ deg. Fig. 7 presents results on automatic computer synthesis of a land-survey SC guidance law for indicated sequence of the observation routes and RM, values of their parameters with using elaborated analytic relations. In Fig. 7 components of vectors $\boldsymbol{\sigma}(t)$, $\boldsymbol{\omega}(t)$ and $\boldsymbol{\varepsilon}(t)$ are marked by different colors – blue color on roll, green on yaw and red on pitch, and modules of vectors $\boldsymbol{\omega}(t)$ and $\boldsymbol{\varepsilon}(t)$ are marked by black color.

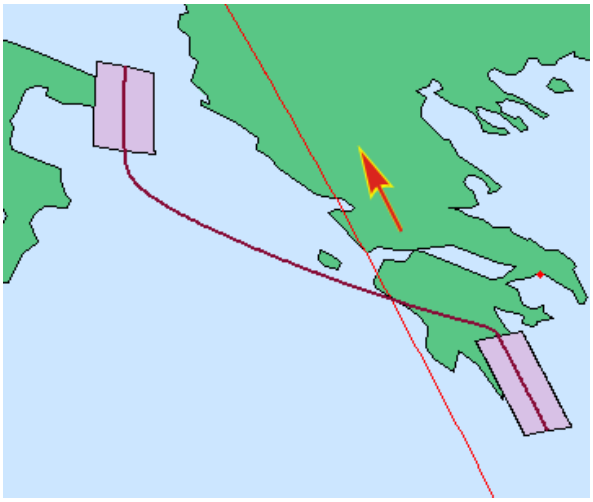

Figure 6. Two observing routes and the RM on a map

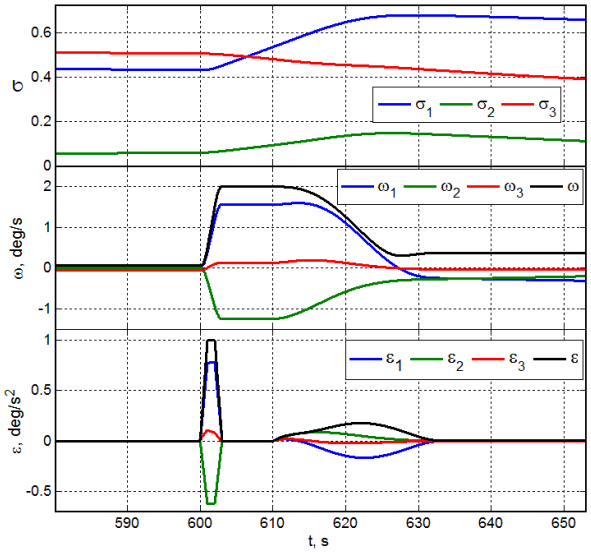

Figure 7. Variations of vectors $\boldsymbol{\sigma}(t)$, $\boldsymbol{\omega}(t)$ and $\boldsymbol{\varepsilon}(t)$

4. A SATELLITE ATTITUDE CONTROL

For the cluster based on four RWs, the principal problem is in distribution of its angular momentum $\mathbf{H}$ and control torque $\mathbf{M}^{\rm r}=-\dot{\mathbf{H}}$ vectors in the BRF between redundant numbers of the reaction wheels. At some simplifications, the problem consists in simultaneous solution of two equations

$$\mathbf{A}_\gamma\,\mathbf{h}=\mathbf{H}\quad\forall\,\mathbf{H}\in\mathbf{R}^3,\mathbf{h}\in\mathbf{R}^4;$$
$$\mathbf{A}_\gamma\,\mathbf{m}=-\mathbf{M}^{\rm r}=\dot{\mathbf{H}}\quad\forall\,\mathbf{M}^{\rm r}\in\mathbf{R}^3,\mathbf{m}\in\mathbf{R}^4. \qquad (5)$$

Unlike standard approach to solving of equations (5) [3] we have applied a scalar function of the cluster tuning for unambiguous distribution of vectors $\mathbf{H}$ and $\mathbf{M}^{\rm r}=-\dot{\mathbf{H}}$ between four RWs by explicit analytical relations. Let us introduce the normed cluster AM vector $\boldsymbol{h}\equiv\{x,y,z\}=\mathbf{H}/\mathrm{h}^{\rm m}=\mathbf{A}_\gamma\mathbf{h}$, where $x=x_1+x_2$, $x_1=C_\gamma(h_1+h_2)$, $x_2=C_\gamma(h_3+h_4)$, $y=S_\gamma(h_1-h_2)$, $z=S_\gamma(h_3-h_4)$; $\mathbf{h}=\{h_p\}$, $h_p=\mathrm{h}_p/\mathrm{h}^{\rm m}$ and $|h_p|\le 1$. Distribution of vector $\mathbf{h}$ is carried out by law

$f_\rho(\mathbf{h}) = \tilde{x}_1 - \tilde{x}_2 + \rho(\tilde{x}_1\tilde{x}_2 - 1) = 0$, $0 < \rho < 1, \rho = \text{const}$;
$\tilde{x}_1 = x_1 / q_y$; $\tilde{x}_2 = x_2 / q_z$, $q_s = (4C_\gamma^2 - s^2)^{1/2}$, $s = y,z$
with notations $a \equiv x/2$, $b \equiv q_y q_z - a^2$ by relations:
(i): $q \equiv q_y + q_z$; $\Delta \equiv (q/\rho)(1-(1-4\rho[(q_y - q_z)a +$
$\rho b]/q^2)^{1/2})$; $x_1 = (x+\Delta)/2$, $x_2 = (x-\Delta)/2$;
(ii) the AM distribution between the RWs in each pair;
(iii) distribution of vector $\mathbf{M}^{\mathrm{r}}$ by explicit formula

$$\mathbf{m} = \{m_p\} = (\{\mathbf{A}_\gamma, \mathbf{a}_f\})^{-1}\{-\mathbf{M}^{\mathrm{r}}, -\mathrm{h}^{\mathrm{m}}\mathrm{Sat}(\phi_\rho, \mu_\rho f_\rho)\}$$

with positive parameters ϕ_ρ, μ_ρ and line $\mathbf{a}_f = [a_{fp}]$ with components

$$a_{f1,2} = \frac{2C_\gamma}{q_y^3}[2C_\gamma^2 \pm S_\gamma^2 h_2(h_1 - h_2)][1 + \rho\frac{C_\gamma(h_3+h_4)}{q_z}];$$

$$a_{f3,4} = \frac{2C_\gamma}{q_z^3}[2C_\gamma^2 \mp S_\gamma^2 h_4(h_3 - h_4)][1 + \rho\frac{C_\gamma(h_1+h_2)}{q_y}].$$

As for problem on in-flight identification of the dry friction torque on the RW rotation axis, we consider one RW only, moreover index p is not used. Simplest model of the RW is presented in normed form $\dot{\Omega}(t) = a(t) - a^{\mathrm{f}}(t)$, $a = m/J_r$, $a^{\mathrm{f}}(t) = a_{\mathrm{o}}^{\mathrm{f}}\,\mathrm{Sign}(\Omega(t))$, acceleration $a^{\mathrm{f}}(t) = \in [-a_{\mathrm{o}}^{\mathrm{f}}, a_{\mathrm{o}}^{\mathrm{f}}]$ describes the effect of the dry friction torque and at known RW inertia moment J_r parameter $a_{\mathrm{o}}^{\mathrm{f}} = m_{\mathrm{o}}^{\mathrm{f}}/J_r = \text{const}$. Assuming $a^{\mathrm{f}}(t) = a^{\mathrm{f}}(t_s) = a_s^{\mathrm{f}} = \text{const}$ $\forall t \in [t_s, t_{s+1})$, the discrete linear Luenberger observer with period T_q is applied in the form $\delta\Omega_s = \Omega_s - \hat{\Omega}_s$; $\hat{a}_{s+1}^{\mathrm{f}} = \hat{a}_s^{\mathrm{f}} + g_2^{\mathrm{f}}\,\delta\Omega_s$; $\hat{\Omega}_{s+1} = \hat{\Omega}_s + (a_s - \hat{a}_s^{\mathrm{f}})\,T_s + g_1^{\mathrm{f}}\,\delta\Omega_s$ for obtaining an estimate $\hat{a}_s^{\mathrm{f}}$ of value a_s^{f}, where parameters g_1^{f} and g_2^{f} are defined by explicit analytical relations. Moreover, discrete estimation of the friction torque is obtained in the form $\hat{m}^{\mathrm{f}}(t_s) = \hat{m}_s^{\mathrm{f}} = J_r\,\hat{a}_s^{\mathrm{f}}$.

The compensation scheme for unloading of RW cluster is based on the following conditions. We compute module I^{m} and unit $\mathbf{e}^{\mathrm{m}}$ for vector of the required pulse of the MD in the BRF, form its variation $\Delta\mathrm{I}^{\mathrm{m}}$ on period T_u^m of the MD pulse-width control and calculate command $\mathbf{M}_k^{\mathrm{cu}} = \{m_{ik}^{\mathrm{cu}}\} = \Delta\mathrm{I}^{\mathrm{m}}\mathbf{e}^{\mathrm{m}}/T_u^m$ by the compensation pulse of the MD torque. This command is sent to the RW cluster only if the MD is switched on. At the time moments t_r, $r \in \mathrm{N}_0$ we determine mutual orientation of units $\mathbf{b}_r$ and $\mathbf{e}_r^{\mathrm{m}}$ into BRF; if $\kappa \equiv |\langle \mathbf{b}_r, \mathbf{e}_r^{\mathrm{m}} \rangle| > \cos(\pi/3)$, then the MD does not switch on during the current period, else we compute vector $\mathbf{L} = \{l_i\} = \Delta\mathrm{I}^{\mathrm{m}}(\mathbf{b}_r \times \mathbf{e}_r^{\mathrm{m}})/B_r$ of required MD torque, durations $\tau_i = T_u^m l_i / \mathrm{l}_m$ (if $\tau_i > T_u^m$, then $\tau_i =: T_u^m \tau_i / \max\{\tau_i\}$) of the MD switch on and signs of l_i by electromagnetic moment on channels.

The inertial ADS (with IMU corrected by STC) has the discrete output signals $\mathbf{\Lambda}_l, \boldsymbol{\omega}_l$ with period T_p. For discrete error quaternion $\mathbf{E}_l = (\mathrm{e}_{0l}, \mathbf{e}_l) = \tilde{\mathbf{\Lambda}}_l^p \circ \mathbf{\Lambda}_l$ angular mismatch vector $\boldsymbol{\varepsilon}_l = -2\mathrm{e}_{0l}\mathbf{e}_l = -\delta\boldsymbol{\phi}_l$ and measured vector $\boldsymbol{\omega}_l$ are filtered with period T_p and then the vector values $\boldsymbol{\varepsilon}_k^{\mathrm{f}}, \boldsymbol{\omega}_k^{\mathrm{f}}$, $k \in \mathrm{N}_0$ are formed for application in the SC attitude digital control law

$$\mathbf{g}_{k+1} = \mathbf{B}\mathbf{g}_k + \mathbf{C}\boldsymbol{\varepsilon}_k^{\mathrm{f}}; \quad \tilde{\mathbf{m}}_k = \mathbf{K}\mathbf{g}_k + \mathbf{P}\boldsymbol{\varepsilon}_k^{\mathrm{f}};$$

$$\mathbf{M}_k^{\mathrm{r}} = \boldsymbol{\omega}_k^{\mathrm{f}} \times \mathbf{G}_k + \mathbf{J}(\mathbf{C}_{ek}\dot{\boldsymbol{\omega}}_\kappa^p + [\mathbf{C}_{ek}\boldsymbol{\omega}_\kappa^p \times]\boldsymbol{\omega}_k^{\mathrm{f}} + \tilde{\mathbf{m}}_k). \quad (6)$$

Here matrix $\mathbf{C}_{ek} = \mathbf{C}_e(t_k)$, $\mathbf{G}_k = \mathbf{J}\boldsymbol{\omega}_k^{\mathrm{f}} + \mathbf{H}_k$ and for $d_u \equiv 2/T_u$, $a \equiv (d_u\tau_1 - 1)/(d_u\tau_1 + 1)$ the diagonal elements of matrices $\mathbf{K}$, $\mathbf{B}$, $\mathbf{C}$, $\mathbf{P}$ are computed in the form $b = (d_u\tau_2 - 1)/(d_u\tau_2 + 1)$; $p = (1-b)/(1-a)$; $c = p(b-a)$ with parameters τ_1, τ_2 and k.

At following the vector $\mathbf{M}_k^{\mathrm{r}} + \mathbf{M}_k^{\mathrm{cu}}$ is "re-calculated" into the RW cluster column $\mathbf{m}_k = \{m_{pk}\}$ of the control torques by the AM explicit distribution between four RWs. The dry friction compensation torques $\hat{m}_k^{\mathrm{f}}$ are added to torques m_{pk} and resulting command torque vector column $\mathbf{m}_k = \{m_{pk}\}$ is fixed on the semi-interval of RWs digital control with period T_u.

5. SIMULATION OF A SATELLITE MOTION

The software system *SIRIUS-S* [4] is intended for designing of guidance, navigation and attitude control systems of the information satellites. The software system contains a dialog monitor, subsystems for modeling, synthesis and analysis, and also technological subsystems for animation of the SC spatial motion and documentation of obtained results. As a result, a design engineer obtains a functional representation of the control system for a designed, for an example land-survey spacecraft with respect to periodicity, productivity and activity of observations, a local spatial resolution, the accuracy of guidance and stabilization of an onboard telescope taking into account disturbances, restrictions and other factors.

Models of the Earth, external environment, the SC structure, its progressive and attitude motions both at the objective- , stereo- and area-observations and at the rotational maneuvers are implemented into *SIRIUS-S* system. These models are based on *Matlab* and allow accurate computing all kinematic parameters of the SC spatial motion and formation of files for the visualization subsystem.

Documented results are represented by scenes of surveying routes in the form of charts, tables, and plots of variations in the SC body coordinates and motions of the executive devices as a function of time, the values of the observation quality characteristics and optimality criterions.

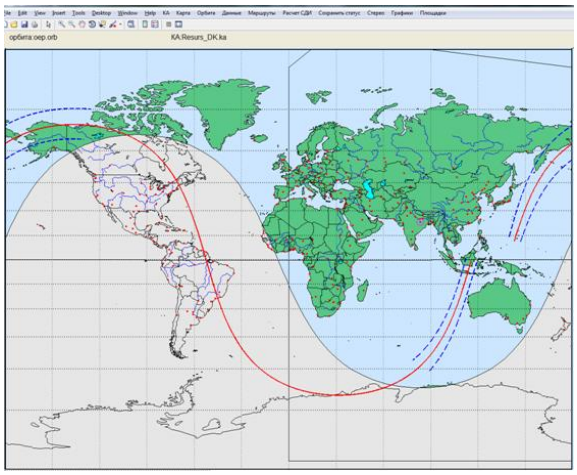

Figure 8. Main dialog window of the *SURIUS-S*

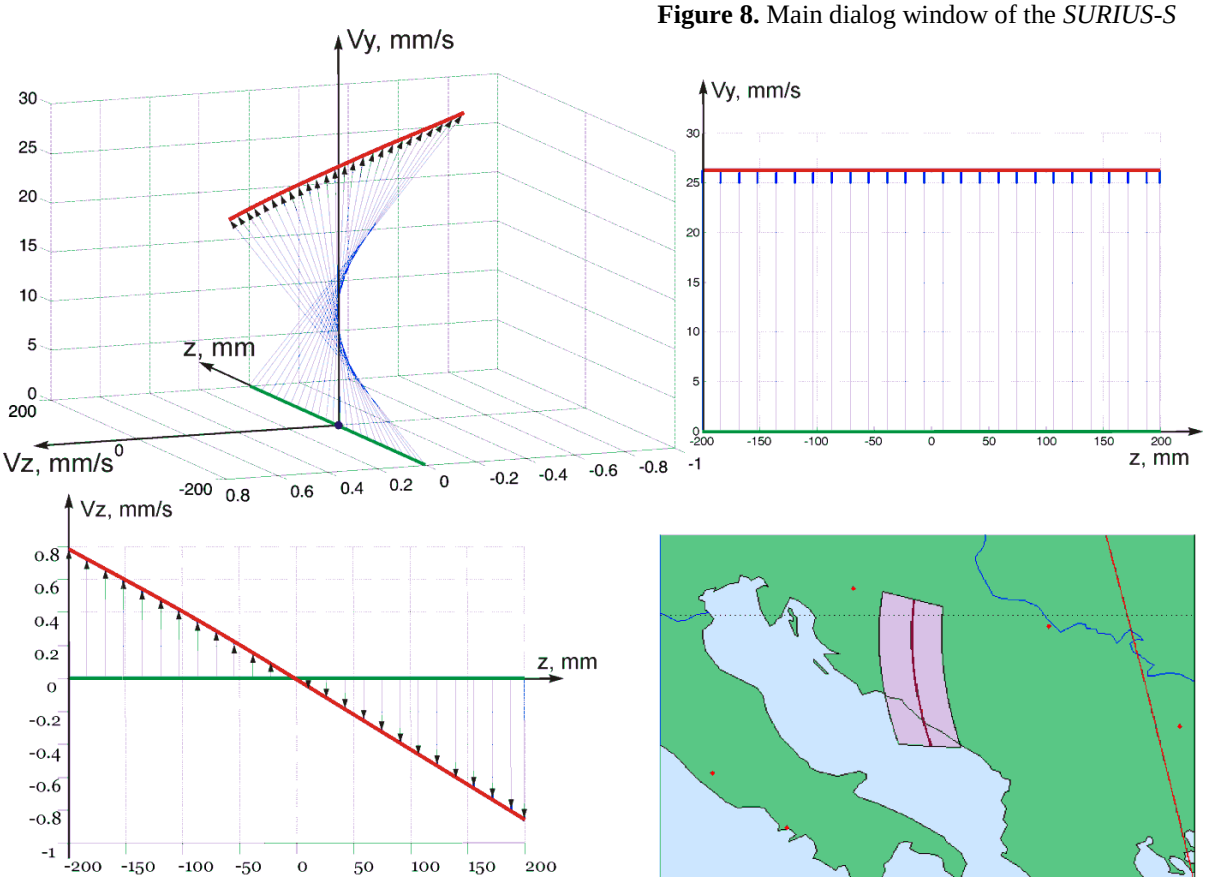

Figure 9. Distribution of the IMV vector $\mathbf{V} = \{V_y, V_z\}$ on the CCD main line at focal plane of telescope

The modeling subsystem contains the following components: the Earth model and electronic maps with the data bases for objects on terrestrial surface; the SC structure model – geometrical and inertial characteristics, parameters of telescope, the measuring and executing devices et al.; ballistic model of the SC mass center motion; models of the SC attitude control – schemes for the Earth surface surveying, computing the routes and rotational maneuvers with general boundary conditions et al. The synthesis and analysis subsystem is intended to carry out the following functions: reflection of the Earth surface maps with the observed objects; reflection of orbit, the SC flight trace and a survey zone, the SC attitude motions at fulfilling the target tasks, verification of their realization at the bounded resources of executing devices; synthesis of algorithms for the SC attitude determination, guidance and attitude control laws; analysis of stability and transient processes into the SC attitude control system at fulfilling given programmed attitude motion; computing of an image motion velocity into given points of the CCD matrix and the attainable local spatial resolution; analysis of variants for the SC control systems on different criterions. The SC motion animation subsystem is a technological software tool. The subsystem was elaborated into *Delphi 7* environ-

ment with the use of *OpenGL* graphic library. The 3D-model of the SC structure has realization into *Blender* environment [5], reflection of its elements is carried out by the *OpenGL* means taking into account the Sun lighting. Here standard procedure is carried out by "sticking on" a texture of the Earth map onto the Earth surface, observed targets are marked and their geographic coordinates are calculated into reference frame of the surveying camera. The SC structure is reflecting together with the trace point, a point of the line-of-sight intersection with the Earth surface and the CCD line projection onto the surface, if a scanning observation is fulfilled at the time moment. The software has possibility to change an image scale and perspective of a scene survey at observation of the Earth rotating surface. The main window of the dialog environment is presented in Fig. 8. Here one can see the top menu, geographic map, the flight trace, bounds of the SC survey zone, and also bounds of light and shade. The dialog is realized by leaked out windows.

Distribution of the IMV vector $\mathbf{V} = \{V_y, V_z\}$ on CCD main line (a work in TDI mode) is presented in Fig. 9. The ED digital control law (6) was researched for a land-survey mini-satellite with mass 400 kg onto the sun-synchronous orbit with altitude 600 km. In Fig. 10 one can see the SC trace (dotted line), first course C_1 at the trace scanning observation into the nadir direction, the line-of-sight track at the SC rotation maneuver (RM) and second course C_2 for next the trace

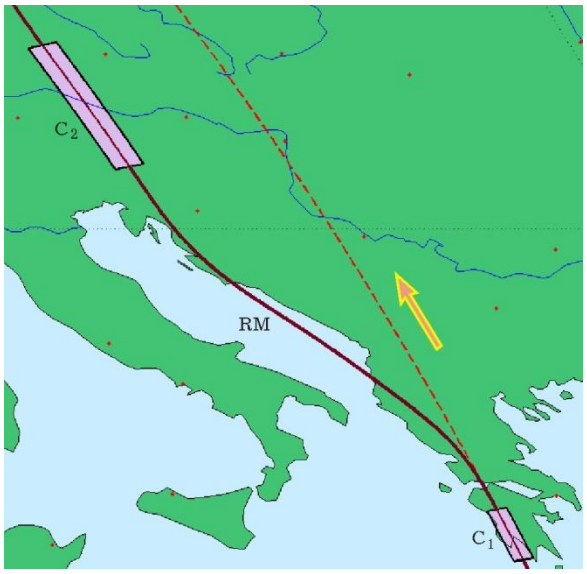

Figure 10. The scanning land-survey by two courses

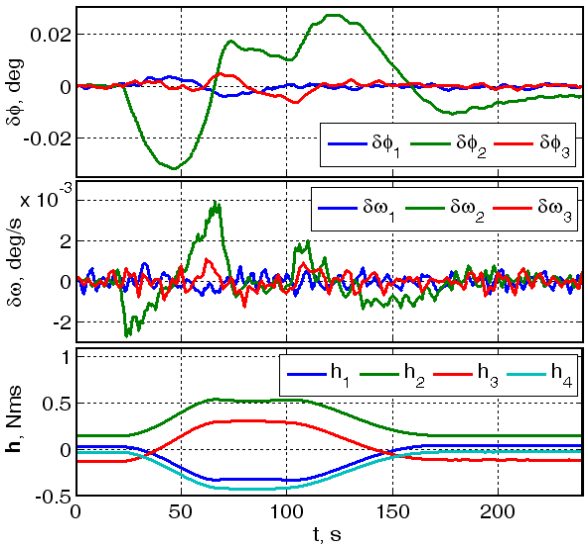

Figure 11. The SC attitude errors and the RW AMs

scanning observation but with the line-of-sight angular deflection on 30 deg at the SC roll channel. The SC attitude guidance law was calculated taking into account restriction $\overline{\omega} = 0.35$ deg/s. The SC attitude errors at 1st course for $t \in [0, 10)$ sec, the RM for $t \in [20, 180)$ sec, 2nd course for $t \in [180, 240]$ sec, and also the RW angular momentums are presented in Fig. 11. Here discrete noise has standard deviation $\sigma^{\mathrm{m}} = 10$ arc sec at the SC attitude measuring by ADS and the time reference $t = 0$ correspond to start of first course (route) by the scanning observation.

Assume that for RW cluster the accumulated AM vector $\mathbf{H}_r^a = \{1,1,1\}$ Nms is given in the BRF and mini-satellite's body is stabilized into the ORF, and for the units $\mathbf{b}(t)$ and $\mathbf{e}_r^{\mathrm{m}} = \{1,1,1\}/\sqrt{3}$ their nearness measure $\kappa \le 1/2$. At values $1^{\mathrm{m}} = 10$ Am^2 and period

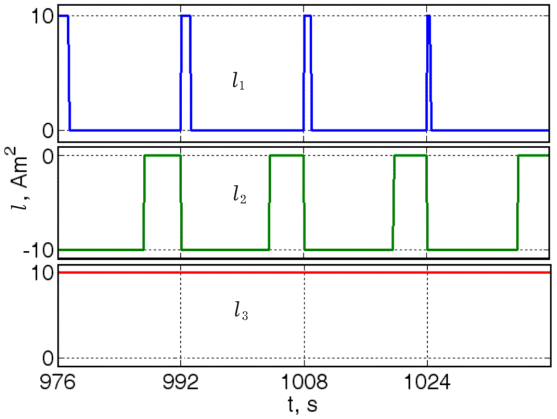

Figure 12. The MD electromagnetic moments

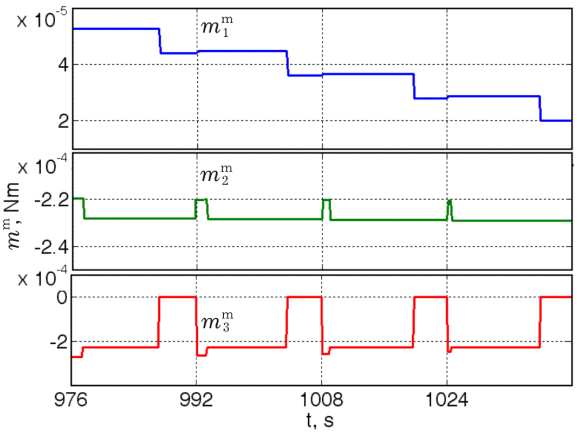

Figure 13. Components of the MD torque vector

Table 1. Surveying method, beginning time and duration of the routes

i	Surveying method	t_i, sec	τ_i, sec
1	*Geo*	475	10
2	*Geo*	575	14
3	*Geo*	620	11
4	*Geo*	660	15
5	*Geo*	690	14
6	*Trace*	735	14.5
7	*Trace*	845	14.5
8	*Trace*	955	14.5
9	*Stereo*	990	23.4
10	*Stereo*	1053	23.5
11	*Smooth*	1120	10
12	*Trace*	1200	8
13	*Trace*	1225	8
14	*Trace*	1250	8

$T_u^m = 16$ sec components $l_i(t)$ of the electromagnetic moment vector $\mathbf{L}(t)$ are presented in Fig 12, and components $\mathbf{M}^{\mathrm{m}}(t) = \{m_i^{\mathrm{m}}(t)\}$ of obtained MD torque vector – in Fig. 13 [6]. Here a time reference is carried out from the time moment by fly-over longitude of ascending node – the orbit rising knot (ORK).

6. ANIMATION OF A SATELLITE MOTION

We note that into field-of-view by the surveying camera simultaneously there are settled down both the Earth rotated surface with marked routes of scanning observation and the SC structure accomplished a spatial motion (6-DOF), the SAPs have possibilities to return with respect to the SC body by 2-DOF universal-joint forks. We have presented the animation results for fulfilling the survey task (Fig. 14, Tab. 1 [6]) for the data: the circle sun-synchronous orbit with inclination 98 deg and a perigee argument 120 deg , the decree Moscow time is 08:58:08 at the ORK passage. Tab. 1 contains a number of the surveying route (i); applied observation method: an orthodromic surveying – *Geo*, a trace surveying – *Trace*, a stereo-surveying – *Stereo*, a surveying with a smoothing of the IMV in the FP – *Smooth*; a time moment of the surveying route beginning (t_i) counted out from the ORK time; a duration (τ_i) of corresponding route. Moreover, routes $i = 1 \div 5$ realize the object observations, routes $i = 6 \div 8$ ensure the area observation, a stereo-survey-ing is carried out by routes $i = 9 \& 10$, curvilinear route $i = 11$ ensures most accurate surveying mode with the IMV smoothing, routes $i = 12 \div 14$ realize tree-divisible object observation. Some frames by animation of the mini-satellite motion at fulfilling of indicated task are presented in Figs. 15 – 16.

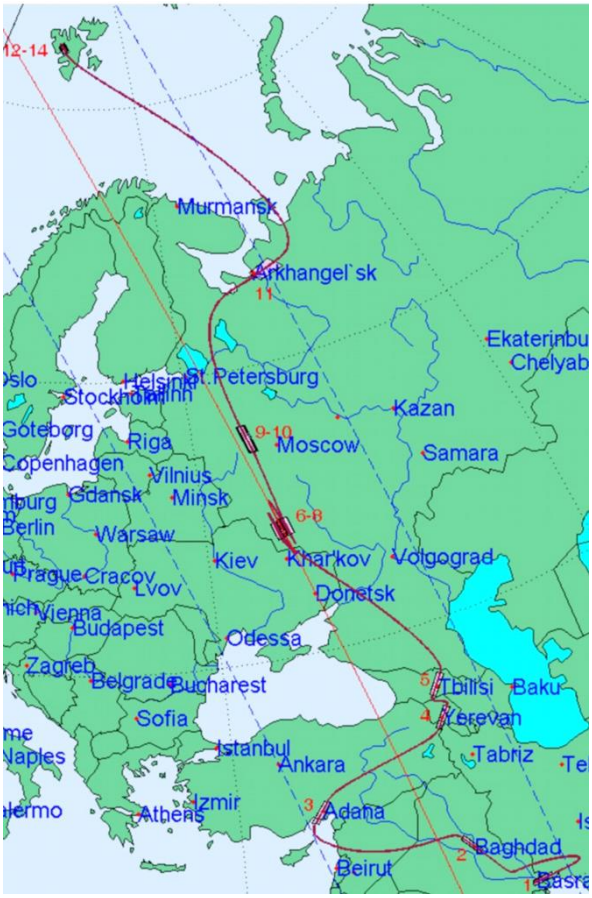

Figure 14. An example of the space survey task

Figure 15. The animation frame of the mini-satellite motion at fulfilling of task

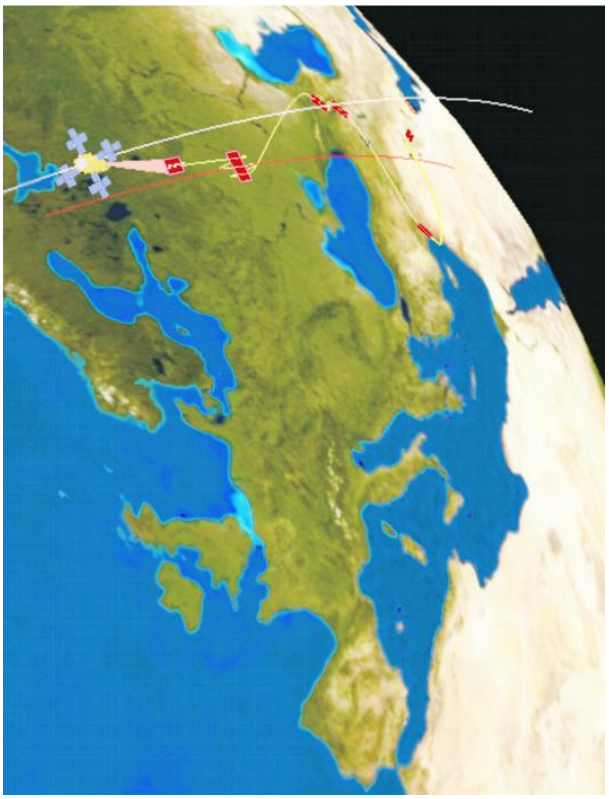

Figure 16. The side animation frame of the mini-satellite spatial motion

In-flight support is provided for the ACS of a land-survey mini-satellite [7, 8]. The support is implemented in terrestrial control flight centre (CFC) in order to ensure the ACS reliability and survivability at faults of onboard devices. For the CFC operators an important problem consists in comprehension of a satellite actual orientation with respect to directions on the standard objects of external space environment (the Earth, Sun, Moon et al.) at emergency situations in the ACS operation when its resources have no possibilities to carry out automatic diagnosis and restoration of the ACS capacity by reconfiguration of the control loop. The computer animation tool allows to eliminate this problem: the SC spatial motions are simultaneously reflected onto two next monitors – on the first one, based on actual telemetric information and on the second one, based on the results of computer simulation of the satellite attitude motion with the same values of parameters, initial conditions and variants of possible faults in the SC control loop. Approximation of a satellite attitude motion by the vector splines makes it possible to simplify computer animation of spacecraft spatial motion.

7. CONCLUSION

We have presented simple methods for attitude guidance and control of the information mini-satellites by cluster of four reaction wheels with digital control and pulse-width controlled magnetic driver applied for the cluster unloading from accumulated angular momentum. We shortly described the developed software environment for simulation, computer-aided designing and in-flight supporting of the attitude guidance and control system for a land-survey mini-satellite with animation of its spatial motion.

8. ACKNOWLEDGMENT

The work was jointly supported RFBR (Russian Foundation for Basic Research) by Grant 14-08-91373 for Samara State Technical University and TUBITAK (The Scientific and Technological Research Council of Turkey) by Grant 113E595 for Istanbul Technical University. The work was also supported Division on the EMMCP of Russian Academy of Sciences, Program for basic research no. 13.

9. REFERENCES

[1] Somova, T.Ye., (2015) "A Vector Polynomial Representation of the Guidance Laws and Animation of a Land-survey Satellite Motion", *Izvestiya of Samara Scientific Centre, Russian Academy of Sciences*, 17 (6(2)), 398-405. ISSN 1990-5378.

[2] Somov, S., Butyrin, S., Somova, T. (2014) "Optimization of Guidance and Attitude Control for Land-survey Mini-satellites", *AIP Conference Proceedings*, 1637, 1018-1027. DOI 10.1063/1.4904676.

[3] Kron, A., St-Amour, A., de Lafontaine, J. (2014) "Four Reaction Wheels Management: Algorithms Trade-off and Tuning Drivers for the PROBA-3 Mission", Proceedings of 19th IFAC World Congress, 19 (1), 9685-9690. DOI 10.3182/20140824-6-ZA-1003.00604.

[4] Somov, Ye.I., Butyrin, S.A., Somov, S.Ye., Somova, T.Ye. (2013) "SIRIUS-S Software Environment for Computer-aided Designing of Attitude Control Systems for Small Information Satellites", Proceedings of 20th Saint Petersburg International Conference on Integrated Navigation Systems, 325-328. ISBN 978-5-91995-020-2.

[5] Mullen, T. (2011) "Introducing Character Animation with Blender", Wiley Publishing. 496 pp. ISBN 978-0-470-4227378.

[6] Somova, T., (2015) "Digital and Pulse-width Attitude Control, Imitation and Animation of Land-survey Mini-satellite", Proceedings of 7th IEEE/AIAA International Conference on Recent Advances in Space Technologies, 765-770. DOI 10.1109/RAST.2015.7208443, ISBN 978-1-4673-7760-7.

[7] Somova, T., (2014) "Application of Simulation and Animation for In-flight Support of the Information Satellite Control Systems", *Control Sciences*, 5, pp. 70-78. ISSN 1819-3161.

[8] Somova, T., (2015) "Algorithms of Simulation and Animation for In-flight Identification and Support of a Land-survey Mini-satellite Control System", Proceedings of 20th International Conference "System Identification and Control Problems", 1078-1089. ISBN 978-5-91450-162-1.

VITAE

Tatyana SOMOVA
was born in 1987 near Baikal lake in Irkutsk, Russia. She graduated the English secondary school no. 18 in Kazan, Russia, and Samara State University of Architecture and Civil Engineering as an engineer on computer designing in 2010. She is currently a junior researcher of department for Navigation, Guidance and Control, and simultaneously a postgraduate student since 2014, at Samara State Technical University, Samara, Russia.